



A new method for isolating turbulent states in transitional stratified plane Couette flow

J. R. Taylor^{1,†}, E. Deusebio¹, C. P. Caulfield^{2,1} and R. R. Kerswell³

¹Department of Applied Mathematics and Theoretical Physics, University of Cambridge, Centre for Mathematical Sciences, Willberforce Road, Cambridge CB3 0WA, UK

²BP Institute, University of Cambridge, Madingley Road, Cambridge CB3 0EZ, UK

³School of Mathematics, University of Bristol, Bristol BS8 1TW, UK

(Received 22 June 2016; revised 22 August 2016; accepted 25 September 2016; first published online 26 October 2016)

We present a new adaptive control strategy to isolate and stabilize turbulent states in transitional, stably stratified plane Couette flow in which the gravitational acceleration (non-dimensionalized as the bulk Richardson number Ri) is adjusted in time to maintain the turbulent kinetic energy (TKE) of the flow. We demonstrate that applying this method at various stages of decaying stratified turbulence halts the decay process and allows a succession of intermediate turbulent states of decreasing energy to be isolated and stabilized. Once the energy of the initial flow becomes small enough, we identify a single minimal turbulent spot, and lower-energy states decay to laminar flow. Interestingly, the turbulent states which emerge from this process have very similar time-averaged Ri , but TKE levels different by an order of magnitude. The more energetic states consist of several turbulent spots, each qualitatively similar to the minimal turbulent spot. This suggests that the minimal turbulent spot may well be the lowest-energy turbulent state which forms a basic building block of stratified plane Couette flow. The fact that a minimal spot of turbulence can be stabilized, so that it neither decays nor grows, opens up exciting opportunities for further study of spatiotemporally intermittent stratified turbulence.

Key words: stratified flows, stratified turbulence, transition to turbulence

1. Introduction

It is well known that fluid flows with a linearly stable laminar state can still undergo a subcritical transition to turbulence and display a wealth of interesting, complex spatiotemporal dynamics which continues to defy understanding. For example, in plane Couette flow where a constant-density fluid of kinematic viscosity ν is sheared

† Email address for correspondence: jrt51@cam.ac.uk

between two parallel boundaries a distance $2h$ apart moving at velocity $\pm U$, there is a Reynolds number, $Re = Uh/\nu = Re_g \simeq 323$, below which the laminar flow is a global attractor but turbulent spots can be triggered transiently (Bottin, Dauchot & Daviaud 1997; Duguet, Schlatter & Henningson 2010). For $Re > Re_g$, the flow can permanently support spatiotemporal intermittency with coexistence of regions of turbulent and laminar flow (Lundbladh & Johansson 1991; Tillmark & Alfredsson 1992; Dauchot & Daviaud 1995). The volume fraction occupied by turbulence increases with Re until it fills the whole domain for $Re > Re_t \simeq 400$ (Duguet *et al.* 2010). Close to but above Re_g , there is a patterned regime where the turbulence arranges itself into regular stripes or bands obliquely oriented to the mean flow and separated by laminar regions (Prigent *et al.* 2002; Barkley & Tuckerman 2005; Duguet *et al.* 2010; Philip & Manneville 2011; Manneville 2012; Duguet & Schlatter 2013). This general picture is repeated across other shear flows undergoing a finite-amplitude transition: for example, certain regimes of Taylor–Couette flow (Coles 1965; Van Atta 1966; Prigent *et al.* 2002) and channel flow (Carlson, Widnall & Peeters 1982; Alavyoon, Henningson & Alfredsson 1986; Fukudome, Iida & Nagano 2009; Tsukahara *et al.* 2005). It also persists under the addition of extra physics such as rotation, Lorentz forces and stratification (Brethouwer, Duguet & Schlatter 2012; Deusebio *et al.* 2014).

Underpinning all this behaviour is the basic phenomenon of a localized finite-amplitude disturbance triggering the growth of a turbulent spot. These spots are never stable, either eventually decaying away if the underlying shear is too low ($Re < Re_g$) or developing into a spatially extended turbulent state such as a turbulent strip ($Re_g < Re < Re_t$) or indeed the whole flow domain ($Re > Re_t$). Observations and numerical calculations indicate that the evolution of a turbulent spot quickly takes on a universal structure independent of the initial disturbance. As a result, much work has been done to try to unravel the dynamics of this growth even though the very fact that the spot is continually evolving has made this difficult (Emmons 1951; Carlson *et al.* 1982; Alavyoon *et al.* 1986; Henningson, Spalart & Kim 1987; Klingmann & Alfredsson 1990; Schumacher & Eckhardt 2001).

Stratification introduces additional parameters, the Richardson number, Ri , which quantifies the relative importance of buoyancy compared to shear, and the Prandtl (or Schmidt) number, $Pr = \nu/\kappa$, the ratio of the fluid viscosity to the scalar diffusivity. Here, we will consider only $Pr = 0.7$, characteristic of the diffusion of heat in air, while varying Ri . Stable density stratification is common in geophysical flows. Despite the very high Re associated with geophysical flows, turbulence is often highly intermittent, as the de-stabilizing influence of vertical shear competes against the stabilizing influence of stratification (e.g. Mahrt 1999). Previous studies have examined the laminar–turbulent transition and intermittency in wall-bounded stratified shear flows (Flores & Riley 2010; García-Villalba & del Álamo 2011; Brethouwer *et al.* 2012; Deusebio *et al.* 2014; Deusebio, Caulfield & Taylor 2015). Figure 1 summarizes the simulations reported in Deusebio *et al.* (2015), with blue circles used to indicate simulations with spatiotemporal intermittency and red squares used to indicate fully turbulent flow.

Motivated by this, we use Ri as a control parameter to study spatiotemporal intermittency using direct numerical simulations (DNS) of stratified plane Couette flow. For simplicity, we consider a single Re , which is nearly three times larger than the critical value for unstratified plane Couette flow, and $Ri \in [0.02, 0.2]$: the baseline simulation with $Ri = 0.02$ is indicated by a filled blue circle in figure 1. In the absence of stratification, flow at this Re would be in the ‘featureless’ turbulence regime. However, stable stratification retards the transition process and the flow

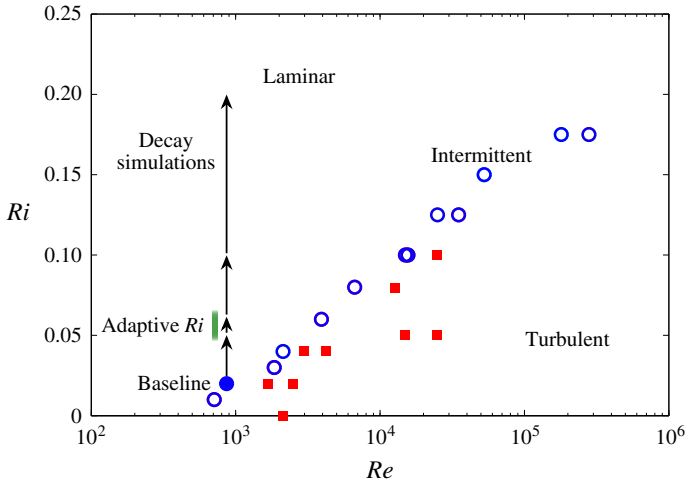


FIGURE 1. Flow regimes in stratified plane Couette flow as a function of Reynolds number, Re , and Richardson number, Ri . All simulations use a Prandtl number $Pr = 0.7$. The simulations reported in Deusebio *et al.* (2015) are indicated with symbols. Blue circles denote simulations with spatiotemporal intermittency and red squares denote fully turbulent simulations. The solid blue circle is the baseline simulation described below in § 2.1. Arrows indicate an abrupt increase in Ri at the start of each decay simulation described in § 2.2, and the green bar indicates the approximate range of Ri seen in the adaptive simulations B, C and D, described in § 2.3.

exhibits spatiotemporal intermittency in the form of patterned turbulence which will be described below. Note that most of the other simulations from Deusebio *et al.* (2015) used a relatively small box size and were unable to distinguish between patterned and irregular intermittent turbulence.

The paper is organized as follows. In § 2.1, we briefly describe the numerical set-up and revisit one of the simulations reported in Deusebio *et al.* (2015) in an intermittent regime, which we use as a baseline simulation. In § 2.2, we describe a series of decay simulations, each of which starts from an initial condition taken from the baseline simulation at $Ri = 0.02$. The decay simulations differ only in the new value of $Ri > 0.02$ subsequently imposed. Section 2.3 then describes a novel strategy to isolate and stabilize a turbulent spot by turning on the dynamic adaptation of Ri in the decay simulation for $Ri = 0.05$. The adaptive control procedure allows us to halt the decay process and isolate stripes and spots that characterize intermittent flows with a supercritical transition. Finally, we end with a brief summary and discussion in § 3.

2. Results

2.1. Set-up

Stratified plane Couette flow is bounded at the top and bottom by flat, rigid plates separated by a distance $2h$. Here, x , y and z will be used to denote the streamwise, wall-normal and spanwise directions, respectively, following the standard convention for Couette and channel flow. The plates move in opposite directions with constant velocity $\mathbf{u} = \pm U\hat{x}$. The walls are held at a fixed temperature, θ , such that the

temperature of the upper wall is $2T$ higher than the temperature of the lower wall. Here, we consider the following non-dimensional incompressible Boussinesq equations with a linear equation of state:

$$\frac{\partial \mathbf{u}}{\partial t} + \mathbf{u} \cdot \nabla \mathbf{u} = -\nabla p + Ri\theta \hat{\mathbf{y}} + \frac{1}{Re} \nabla^2 \mathbf{u}, \quad (2.1)$$

$$\frac{\partial \theta}{\partial t} + \mathbf{u} \cdot \nabla \theta = \frac{1}{RePr} \nabla^2 \theta, \quad (2.2)$$

$$\nabla \cdot \mathbf{u} = 0, \quad (2.3)$$

where

$$Re := Uh/\nu, \quad Ri := |\mathbf{g}|\alpha Th/U^2, \quad Pr := \nu/\kappa, \quad (2.4a-c)$$

$\mathbf{g} = -g\hat{\mathbf{y}}$ is the acceleration due to gravity which acts in the $-y$ direction, ν is the kinematic viscosity, κ is the thermal diffusivity, α is the thermal expansion coefficient, and p is the non-dimensional pressure.

Periodic boundary conditions are applied in x and z . The numerical code uses a pseudo-spectral method in x and z and second-order finite differences to calculate derivatives in the y direction. The time stepping algorithm is a mixed implicit/explicit scheme using the third-order Runge–Kutta and Crank–Nicolson methods. Further details of the problem configuration and numerical method can be found in Deusebio *et al.* (2015).

One of the simulations reported by Deusebio *et al.* (2015) is chosen as our ‘baseline’ simulation (filled blue circle in figure 1). This simulation has $Re = 865$, $Ri = 0.02$ and $Pr = 0.7$. Although Re is among the lowest considered by Deusebio *et al.* (2015), it is still sufficiently high to be in the ‘fully turbulent’ regime for unstratified plane Couette flow ($Re \gtrsim 400$) (Duguet *et al.* 2010). This case was chosen as our baseline since the modest resolution allows us to use a very large domain in the streamwise and spanwise directions, with $L_x = 64\pi h$ and $L_z = 32\pi h$. The simulation uses 1024 gridpoints in the x and z directions and 64 points in y , with gridpoints clustered near both walls. As discussed by Deusebio *et al.* (2015), the large domain size reduces temporal intermittency of the flow and provides robust statistics.

Figure 2(b) shows the streamwise velocity at $y = -0.5h$, the horizontal plane halfway between the lower wall and the centreline. Turbulent and laminar regions develop in inclined bands reminiscent of those seen at lower Reynolds numbers in transitional plane Couette flow (Prigent *et al.* 2002). Deusebio *et al.* (2015) described a method for identifying local turbulent and laminar regions and defined the ‘turbulent fraction’, γ , as the fraction of the total domain occupied by turbulent flow. For sufficiently large Re and small Ri , the flow is fully turbulent with $\gamma = 1$ (red squares in figure 1). For sufficiently small Re and large Ri , intermittent flow is seen with $0 < \gamma < 1$ (blue circles in figure 1). For the baseline simulation, $\gamma = 0.64$ (solid circle in figure 1).

2.2. Decay simulations

In the first set of simulations, we varied the strength of the stable stratification by abruptly increasing Ri . Each simulation was initialized from the baseline simulation described above with $Re = 865$ and $Ri = 0.02$ with a state obtained at statistical equilibrium. The decay simulations are indicated in figure 1 as vertical arrows ending at the new Richardson number. For convenience, $t = 0$ will correspond to the time when Ri is abruptly increased. Since Ri multiplies the buoyancy term in the

Isolating turbulent states in stratified plane Couette flow

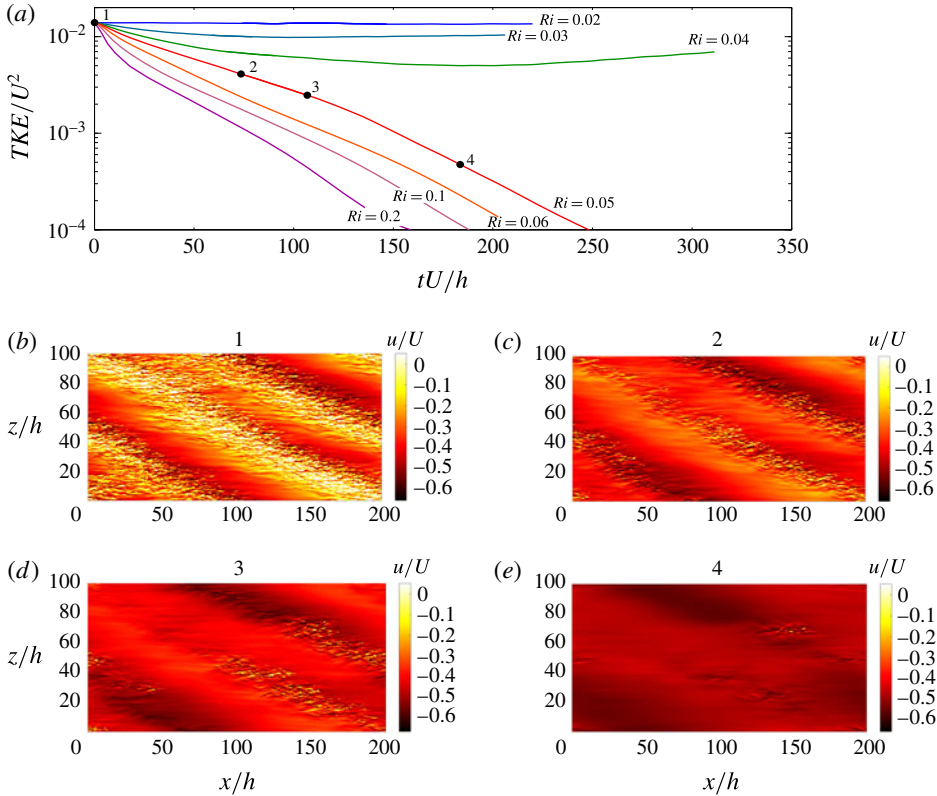


FIGURE 2. (a) Time series of the turbulent kinetic energy (TKE) in the decay simulations. Each simulation starts from the same initial state labelled 1. The Richardson number in each simulation is labelled. (b)–(e) Horizontal slices of the streamwise velocity at $y = -0.5h$ at various times in the simulation with $Ri = 0.05$. The corresponding times are indicated with dots and numbered in panel (a). The first time (b) shows the velocity in the baseline simulation that was used to initialize the decay simulations. In this simulation spatiotemporal intermittency takes the form of a repeating pattern of bands (or stripes) of turbulence inclined with respect to the spanwise direction.

non-dimensional vertical momentum equation, increasing Ri is equivalent to increasing the gravitational acceleration, i.e. heavy fluid becomes heavier and light fluid becomes lighter.

Figure 2(a) shows the time evolution of the turbulent kinetic energy, $TKE := \langle \mathbf{u}' \cdot \mathbf{u}' \rangle / 2$, where $\langle \cdot \rangle$ denotes a volume average and primes denote a departure from this average, i.e. $\mathbf{u}' := \mathbf{u} - \langle \mathbf{u} \rangle$. In four cases with $Ri \geq 0.05$, the TKE decays in time at an approximately exponential rate, and the rate of decay increases with Ri . Eventually all simulations with $Ri \geq 0.05$ reach a fully laminar state. When $Ri = 0.03$ and $Ri = 0.04$, the TKE decays during a transient period and partially recovers, but remains below the initial value. For comparison, a continuation of the baseline case with $Ri = 0.02$ is also shown.

The decay process does not proceed uniformly in space, but instead turbulence persists in localized ‘pockets’ contained within receding turbulent bands, qualitatively similar to what has been seen in previous simulations of decaying unstratified turbulence (Manneville 2011). Figure 2(b)–(e) shows four snapshots of the streamwise

velocity at $y = -0.5h$ in the decay simulation with $Ri = 0.05$. The corresponding times are indicated using dots in figure 2(a). Highly localized patches of turbulence can be seen at times labelled 3 and 4, while the rest of the flow is nearly laminar.

2.3. Adaptive Ri simulations

In order to examine further the influence of stratification on the flow near the laminar-turbulent transition, we have developed a procedure using the Richardson number, Ri , as an adaptive control parameter. To our knowledge, this is the first time that Ri has been used to control the level of turbulence in a stratified flow. The procedure allows us to isolate turbulent states progressively closer to the relaminarization boundary. The adaptive procedure changes Ri based on the rate of change of TKE. Let t_0 correspond to the time M time steps before the current time, t , and let $TKE(t_0)$ and $TKE(t)$ be the TKE at these times. The TKE decay time scale, τ , between times t_0 and t is

$$\tau := \frac{-(t - t_0)}{\ln\left(\frac{TKE(t)}{TKE(t_0)}\right)} \quad (2.5)$$

and the Richardson number, $Ri(t)$, is then set as

$$Ri(t) := Ri(t_0) - c \frac{t - t_0}{\tau}, \quad (2.6)$$

where $Ri(t_0)$ was the previous value at t_0 , and c is a control parameter that will be discussed later. The adaptive Ri procedure acts to maintain a roughly constant value of the TKE. The turbulent fraction and TKE level are sensitive to Ri (Deusebio *et al.* 2015). During periods where TKE decreases in time ($\tau > 0$), the adaptive procedure will decrease Ri , which has the ultimate effect of increasing the TKE, thus leading to the possibility of ‘controlling’ the turbulence at a non-trivial level. Mathematically, if Ri was adjusted every time step, equations (2.5) and (2.6) are a finite difference approximation to imposing the extra dynamical constraint

$$\frac{d}{dt} \left[Ri(t) + c \ln\left(\frac{TKE}{TKE_0}\right) \right] = 0, \quad (2.7)$$

to the Boussinesq equations and TKE_0 is an arbitrary constant energy. Note that $c = 0$ recovers the Boussinesq equations with constant Ri .

In the adaptive Ri simulations, we updated Ri using (2.6) every $M = 20$ time steps and set $c = 0.1$. The value of M was chosen to reduce the computational cost of this procedure while ensuring that Ri is adjusted sufficiently often to keep pace with any change in the TKE decay rate. In practice, the time between Ri adjustment steps is always less than one advective unit, $t - t_0 < h/U$. The sensitivity of the results to the choice of c will be examined later. We have used the adaptive Ri procedure to isolate turbulent states during various stages of the decay process. We saved three-dimensional flow fields at various times during the decay simulation with $Ri = 0.05$, indicated by dots in figure 3(a). Each of these was then used as an initial condition for an adaptive Ri simulation. To ensure continuity, Ri was initialized to 0.05 in the adaptive Ri simulations.

Time series of the TKE from the adaptive Ri simulations are shown in dashed lines in figure 3(a). The decay simulation with $Ri = 0.05$ is shown for reference (solid line).

Isolating turbulent states in stratified plane Couette flow

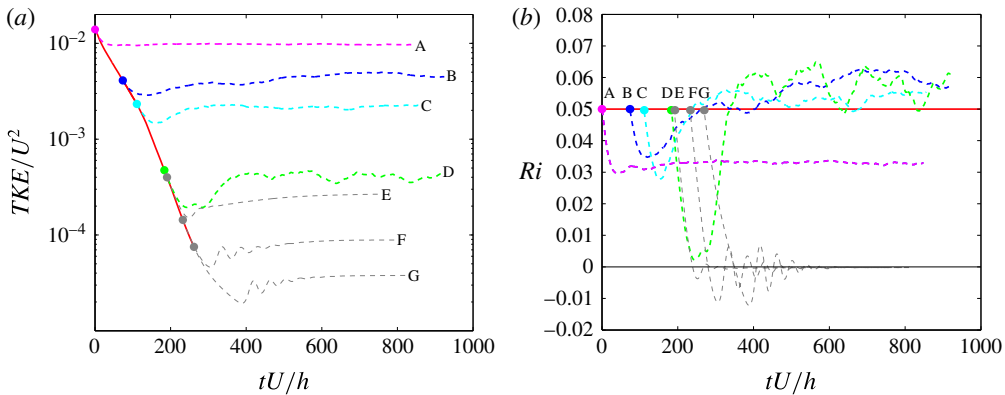


FIGURE 3. (a) Time series of the turbulent kinetic energy (TKE) in the adaptive Ri simulations. The simulations are initialized from various times in the $Ri = 0.05$ decay simulations as indicated by coloured dots. (b) Time series of the Richardson number, Ri , for each of the adaptive Ri simulations using the control scheme described in the text. The solid red line indicates $Ri = 0.05$ from the decay simulation. The start time of each simulation is indicated with a coloured dot, and the colours and labels are the same as in panel (a).

The simulations with adaptive Ri are each labelled with a letter (A–G). In simulations labelled A–D, the TKE continues to decrease at the start of the adaptive simulation, but soon reaches a quasi-steady state. Simulations initialized later in the decay process have quasi-steady states with lower TKE. Time series of Ri in the adaptive simulations are shown in figure 3(b). In all cases Ri reaches a quasi-steady state after an initial drop – mirroring the TKE. Interestingly, the quasi-steady value of Ri in cases B, C and D falls in the same range, $Ri \simeq 0.05$ – 0.06 , despite very different values of the TKE in these simulations. Simulation A has a smaller quasi-steady value of $Ri \simeq 0.03$. For context, the approximate range of Ri in the quasi-steady state for simulations B, C and D is indicated as a green band in figure 1.

Simulation D is the lowest level of TKE that we have been able to reach using this procedure. In simulations E–G, the flow nearly relaminarizes during the adaptive Ri simulation. In this regime, Ri oscillates and eventually becomes negative (figure 3b), while the flow develops into a series of streamwise-independent rolls (not shown) corresponding closely to slightly supercritical, sheared Rayleigh–Bénard convection (Clever, Busse & Kelly 1977; Kelly 1977). There are dramatic differences in the character of the flow and the value of the steady-state Ri in simulations D and E, implying that the flow in simulation D is close to the relaminarization boundary.

The streamwise velocity at $y = -0.5h$ is shown for four adaptive Ri simulations in figure 4. Each snapshot corresponds to the end of the adaptive Ri simulation, as labelled in figure 3(a). Simulation A was initialized directly from the baseline simulation (magenta dot) with $Ri = 0.05$ and the TKE decreases slightly at the start of the simulation. Turbulent/laminar bands are still prominent features of simulation A, and the laminar regions are more coherent than in the baseline simulation (compare figure 2b and figure 4 simulation A). In the other extreme, simulation D has a single turbulent spot. This spot persists throughout the adaptive Ri simulation, slowly migrating around the domain. Simulations B and C have multiple turbulent spots resembling the one seen in simulation D. In simulation B some of the spots appear to join together, with some indications of short inclined bands of turbulence.

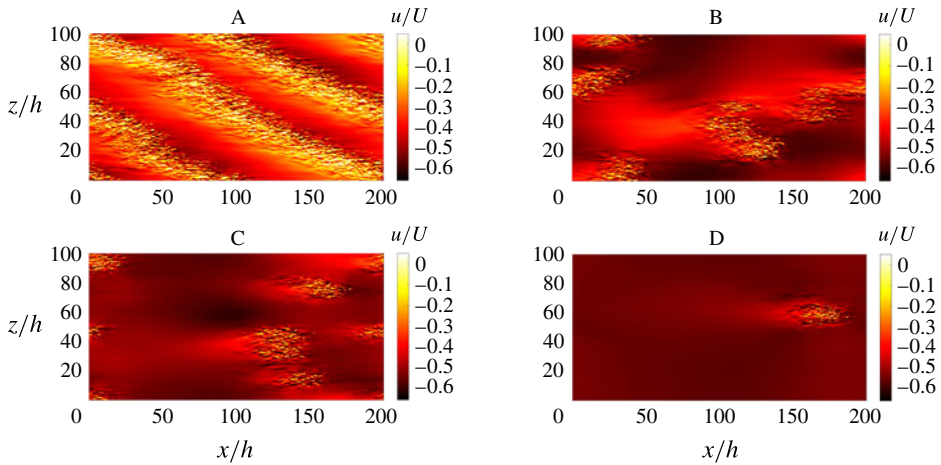


FIGURE 4. Horizontal slices of the streamwise velocity at $y = -0.5h$ at the end of the adaptive Ri simulations. Labels are the same as in figure 3.

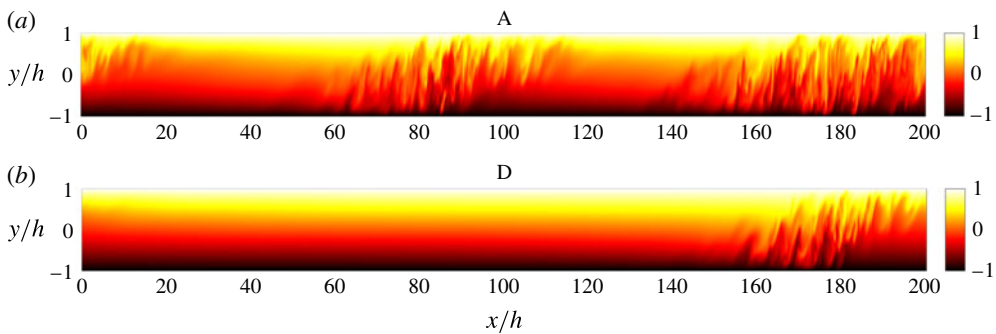


FIGURE 5. Non-dimensional temperature (θ/T) on vertical slices passing through $z = 60h$ for simulations A (a) and D (b). The simulation names are the same as in figures 3 and 4.

The turbulent structures in the isolated turbulent spot are qualitatively similar to the structures in the turbulent stripes. Figure 5 shows vertical slices of the temperature field from simulations A and D illustrating these two regimes. Turbulence in the stripes and spot spans the gap between the lower and upper plates, and is inclined in the direction of plate motion. Small regions with an unstable density arrangement (heavy over light) occur in the turbulent patch. Features reminiscent of developing Kelvin–Helmholtz billows appear on the flanks of the turbulent patches, for example between $60 \leq x/h \leq 80$ in simulation A and $150 \leq x/h \leq 170$ in simulation D (note that the aspect ratio is highly stretched).

To examine the sensitivity of our results to details of the adaptive Ri procedure, we continued simulation D (exhibiting a single turbulent spot) with various values of the adjustment coefficient, c , including a case with $c = 0$ when Ri is held fixed. Time series of the TKE and Ri are shown in figure 6. When $c = 1$, the TKE remains close to constant in time, but Ri exhibits large, high-frequency oscillations. In contrast, when Ri is held fixed ($c = 0$), the TKE undergoes large low-frequency oscillations in time. In this uncontrolled simulation the turbulent spot first grows, splits into two spots, and

Isolating turbulent states in stratified plane Couette flow

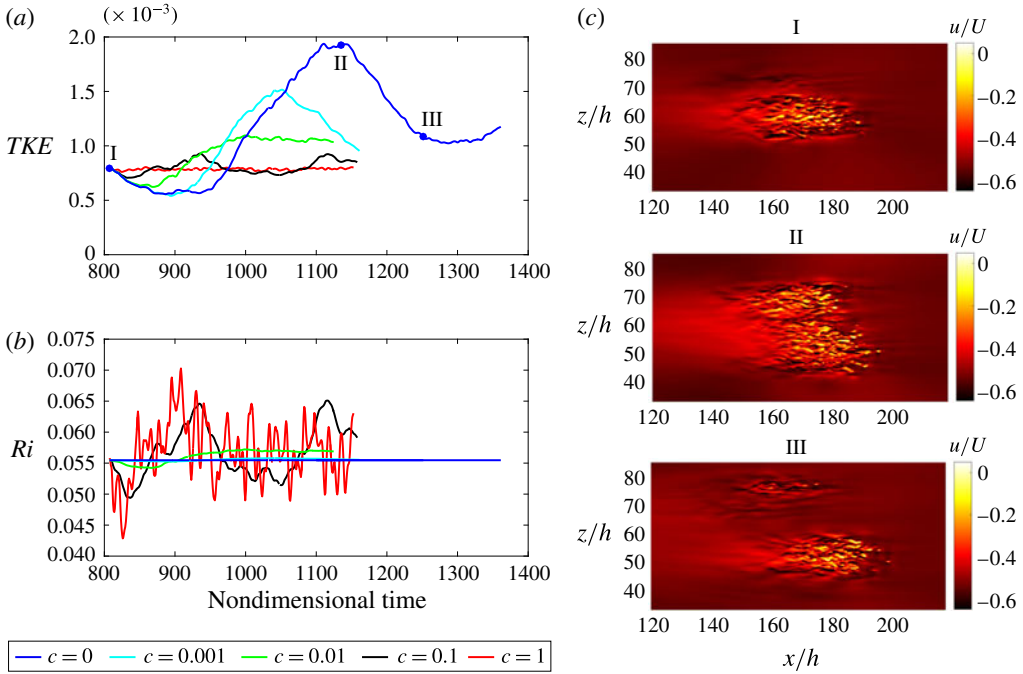


FIGURE 6. Dependence of the TKE (a) and Richardson number (b) on the choice of the coefficient, c , in (2.6). Each simulation is started from the end of simulation D with a single controlled turbulent spot. (c) Visualizations of the streamwise velocity from an uncontrolled simulation ($c=0$) are shown for the times indicated in blue dots in panel (a).

one of these spots decays (figure 6c). The remaining spot looks remarkably similar to the controlled spot from which the simulation was started, more than 400 advective time units earlier (compare times labelled I and III). This suggests that the controlled spot is at least qualitatively representative of the uncontrolled system. The intermediate values, $c=0.1$ and $c=0.01$, represent a trade-off between larger oscillations in Ri and TKE, respectively.

A natural question to ask is whether the captured turbulent spot obtained using the adaptive control procedure is sensitive to the initial conditions. That is, does the flow retain some ‘memory’ of the simulation with decaying stratified turbulence from which it was started? To address this question, we ran an additional simulation initialized with a localized ‘seed’ following the procedure of Lagha & Manneville (2007). Specifically, we started with the velocity from a simulation of unstratified plane Couette flow at the same Reynolds number in the featureless turbulence regime. The initial velocity was then formed by multiplying the unstratified velocity field by a Gaussian function of x and z ,

$$\mathbf{u}(\mathbf{x}, t = 0) = \mathbf{u}_{Ri=0}(\mathbf{x})e^{-(x^2+z^2)/S}, \quad (2.8)$$

where $S = 2h^2$. Note that this seed is significantly smaller than the turbulent spot seen in simulation D. The seed was allowed to develop with $Ri = 0$ for 35 advective time units, after which point, the adaptive procedure was started with $c = 0.1$. Although the Richardson number was started from $Ri = 0$, it converged towards approximately the same value seen in simulations B, C and D, and the flow developed into a single

turbulent spot that appeared extremely similar in structure to the one in simulation D. This result implies that the turbulent spot is not sensitive to the initialization procedure. When the adaptive procedure was started without first allowing the seed to grow, the increase in stratification caused the flow to relaminarize. This supports the idea that the turbulent spot captured in simulation D is close to the minimal energy turbulent attractor, the lowest-energy turbulent state that can be maintained using the adaptive Ri procedure.

3. Discussion

We have examined intermittent stratified plane Couette flow using direct numerical simulations. While the Reynolds number was kept fixed, the Richardson number, Ri , was used as a control parameter, allowing us to probe the dynamics of intermittent stratified turbulence in this geometry. We have considered two sets of simulations. In the first set of simulations, Ri is abruptly increased relative to a control simulation. For sufficiently large values of Ri , the flow relaminarizes. However, in these simulations, localized patches of turbulence persist into the decay period until the flow becomes fully laminar. This result is qualitatively similar to Manneville (2011), who found breakup of turbulent bands in decaying unstratified plane Couette flow.

Next, we describe a new method to isolate flow structures at very low turbulent energy using Ri as an adaptive control parameter. The method adjusts Ri based on the time rate of change in the turbulent kinetic energy (TKE), increasing Ri when the TKE is increasing and lowering Ri when the TKE is decreasing. The adaptive control procedure acts to stabilize the flow close to the initial energy level. By starting the adaptive procedure at various times during a simulation of decaying stratified turbulence, we are able to isolate a variety of low-energy flow structures, including spots and short stripes of turbulence.

When the Richardson number changes through the control procedure introduced here, the buoyancy of the fluid changes everywhere in the domain instantaneously. It is difficult to imagine a means to change the density of a real fluid in a similar way by changing its temperature or salinity. However, a change in buoyancy could be interpreted as a change in the gravitational acceleration. An analogue laboratory experiment would measure the change in TKE within a given time window and accelerate the entire Couette flow apparatus up or down so as to change the fluid buoyancy instantaneously everywhere throughout the flow. Although it would be difficult to implement this system in a practical laboratory experiment, it provides a physical interpretation of the control procedure.

The lowest-energy turbulent structure that we are able to identify using the adaptive control procedure consists of a single isolated turbulent spot in an otherwise laminar flow. Qualitatively, this stabilized spot is very similar to the spots seen previously in unstratified transitional flows, and it seems reasonable to assume that they are closely related. Studying this stabilized spot then offers an exciting opportunity to probe the dynamics seen. However, confirming a connection is not as simple as examining the $c \rightarrow 0$ limit, because the fluctuations in energy become larger as c decreases, until eventually the spot becomes uncontrollable at some small but finite c (see figure 6).

The scheme to adapt Ri based on the time rate of change of TKE is somewhat arbitrary, and other choices could be made. For example, it might be possible to control a turbulent spot in unstratified flow using the Reynolds number as a control parameter. One could use this technique to explore the dynamics of multiple interacting controlled spots. For example, if a simulation were initialized with several

isolated turbulent spots, would they coalesce into stripes and eventually form patterns? If so, do the properties of the turbulent spot provide insight into properties of patterned turbulence such as the width of the turbulent bands?

Another interesting issue is how the stabilized spot in the controlled system – the Boussinesq equations augmented by the constraint (2.7)) with $Ri(t)$ now a dynamic variable – is related to the laminar–turbulent boundary or ‘edge’ (Itano & Toh 2001; Skufca, Yorke & Eckhardt 2006) in the uncontrolled Boussinesq equations with, say, the required fixed value of Ri defined as \bar{Ri} , the long-time average of $Ri(t)$ (a reasonable but not unique choice to link the controlled system with variable $Ri(t)$ and the uncontrolled system with fixed Ri). In the controlled system, the spot is a stable low-energy state and must therefore sit ‘above’ the edge (i.e. not in the laminar basin of attraction) but presumably still close to it. The edge for the controlled system has an extra dimension in phase space compared to that for the uncontrolled system due to $Ri(t)$ being an extra dynamic variable. Projecting the edge in the controlled system down onto the hyperplane with fixed $Ri = \bar{Ri}(t)$ might produce a good estimate for the edge in the uncontrolled system provided the fluctuations in $Ri(t)$ are not too large compared to $\bar{Ri}(t)$. However, it is unclear where the projected stabilized spot solution will land in phase space relative to the uncontrolled system edge: i.e. it could be inside, outside or even on it, and so the control procedure is not a direct competitor to bisection-based edge tracking (Itano & Toh 2001; Skufca *et al.* 2006), which endeavours to work *on* the edge.

In this paper we have only considered a single Reynolds number, $Re = Uh/\nu = 865$. Although this Reynolds number is large enough to support fully developed turbulence in the unstratified limit, it is much smaller than typical values in geophysical and industrial flows. One consequence of the moderate Reynolds number is that the Richardson number associated with intermittent flow is also modest. Deusebio *et al.* (2015) found intermittent behaviour at much higher Reynolds numbers for sufficiently large Richardson number, which is also consistent with previous work (e.g. Flores & Riley 2010; García-Villalba & del Álamo 2011; Brethouwer *et al.* 2012). The fate of the laminar–turbulent transition boundary in the limit as $Re \rightarrow \infty$ is one of the most important open problems in stratified turbulence. Knowing whether there is a finite ‘critical’ value of Ri above which turbulence cannot persist as $Re \rightarrow \infty$ would be of great use in parameterizing turbulence and mixing in ocean, atmosphere, and climate models.

One of the difficulties with answering this question is the rapid increase in computational cost with increasing Re . Very close to the transition boundary, where stratification suppresses energetic turbulence and localizes turbulent patches, the flow might be more accessible to DNS. However, this accessible region narrows in parameter space as $Re \rightarrow \infty$ (Deusebio *et al.* 2015), making it difficult to locate the transition boundary. Here, too, our adaptive control technique might be helpful, since the long-time average of $Ri(t)$ needed to maintain a low perturbation energy level as Re increases should be a good predictor for this boundary.

Acknowledgements

The EPSRC grant EP/K034529/1 entitled ‘Mathematical Underpinnings of Stratified Turbulence’ is gratefully acknowledged for supporting the research presented here. We thank P. F. Linden, S. B. Dalziel and the rest of the MUST team for many helpful discussions. We also thank three anonymous referees for their helpful comments. Data for the initial conditions and simulation output are made available at <https://doi.org/10.17863/CAM.5913>.

References

- ALAVYOON, F., HENNINGSON, D. S. & ALFREDSSON, P. H. 1986 Turbulent spots in plane Poiseuille flow—flow visualization. *Phys. Fluids* **29** (4), 1328–1331.
- BARKLEY, D. & TUCKERMAN, L. S. 2005 Computational study of turbulent laminar patterns in Couette flow. *Phys. Rev. Lett.* **94** (1), 014502.
- BOTTIN, S., DAUCHOT, O. & DAVIAUD, F. 1997 Intermittency in a locally forced plane Couette flow. *Phys. Rev. Lett.* **79** (22), 4377–4380.
- BRETHOUWER, G., DUGUET, Y. & SCHLATTER, P. 2012 Turbulent–laminar coexistence in wall flows with Coriolis, buoyancy or Lorentz forces. *J. Fluid Mech.* **704**, 137–172.
- CARLSON, D. R., WIDNALL, S. E. & PEETERS, M. F. 1982 A flow-visualization study of transition in plane Poiseuille flow. *J. Fluid Mech.* **121**, 487–505.
- CLEVER, R. M., BUSSE, F. H. & KELLY, R. E. 1977 Instabilities of longitudinal convection rolls in Couette flow. *Z. Angew. Math. Phys.* **28** (5), 771–783.
- COLES, D. 1965 Transition in circular Couette flow. *J. Fluid Mech.* **21** (03), 385–425.
- DAUCHOT, O. & DAVIAUD, F. 1995 Finite amplitude perturbation and spots growth mechanism in plane Couette flow. *Phys. Fluids* **7** (2), 335–343.
- DEUSEBIO, E., BRETHOUWER, G., SCHLATTER, P. & LINDBORG, E. 2014 A numerical study of the unstratified and stratified Ekman layer. *J. Fluid Mech.* **755**, 672–704.
- DEUSEBIO, E., CAULFIELD, C. P. & TAYLOR, J. R. 2015 The intermittency boundary in stratified plane Couette flow. *J. Fluid Mech.* **781**, 298–329.
- DUGUET, Y. & SCHLATTER, P. 2013 Oblique laminar-turbulent interfaces in plane shear flows. *Phys. Rev. Lett.* **110** (3), 034502.
- DUGUET, Y., SCHLATTER, P. & HENNINGSON, D. S. 2010 Formation of turbulent patterns near the onset of transition in plane Couette flow. *J. Fluid Mech.* **650**, 119–129.
- EMMONS, H. W. 1951 The laminar-turbulent transition in a boundary layer – Part I. *J. Aero. Sci.* **18** (7), 490–498.
- FLORES, O. & RILEY, J. J. 2010 Analysis of turbulence collapse in stably stratified surface layers using direct numerical simulation. *Boundary-Layer Meteorol.* **129** (2), 241–259.
- FUKUDOME, K., IIDA, O. & NAGANO, Y. 2009 The mechanism of energy transfer in turbulent Poiseuille flow at very low Reynolds number. In *Proceedings of 6th International Symposium on Turbulence and Shear Flow Phenomena*, pp. 471–476. Begel House.
- GARCÍA-VILLALBA, M. & DEL ÁLAMO, J. C. 2011 Turbulence modification by stable stratification in channel flow. *Phys. Fluids* **23** (4), 045104.
- HENNINGSON, D., SPALART, P. & KIM, J. 1987 Numerical simulations of turbulent spots in plane Poiseuille and boundary-layer flow. *Phys. Fluids* **30** (10), 2914–2917.
- ITANO, T. & TOH, S. 2001 The dynamics of bursting process in wall turbulence. *J. Phys. Soc. Japan* **70**, 703–716.
- KELLY, R. E. 1977 The onset and development of Rayleigh–Bénard convection in shear flows: a review. *Physico-Chem. Hydrodyn.* **1**, 65–79.
- KLINGMANN, B. G. B. & ALFREDSSON, P. H. 1990 Turbulent spots in plane Poiseuille flow – measurements of the velocity field. *Phys. Fluids A* **2** (12), 2183–2195.
- LAGHA, M. & MANNEVILLE, P. 2007 Modeling of plane Couette flow. I: large scale flow around turbulent spots. *Phys. Fluids* **19** (9), 094105.
- LUNDBLADH, A. & JOHANSSON, A. V. 1991 Direct simulation of turbulent spots in plane Couette flow. *J. Fluid Mech.* **229**, 499–516.
- MAHRT, L. 1999 Stratified atmospheric boundary layers. *Boundary-Layer Meteorol.* **90** (3), 375–396.
- MANNEVILLE, P. 2011 On the decay of turbulence in plane Couette flow. *Fluid Dyn. Res.* **43** (6), 065501.
- MANNEVILLE, P. 2012 On the growth of laminar–turbulent patterns in plane Couette flow. *Fluid Dyn. Res.* **44** (3), 031412.
- PHILIP, J. & MANNEVILLE, P. 2011 From temporal to spatiotemporal dynamics in transitional plane Couette flow. *Phys. Rev. E* **83** (3), 036308.

Isolating turbulent states in stratified plane Couette flow

- PRIGENT, A., GRÉGOIRE, G., CHATÉ, H., DAUCHOT, O. & VAN SAARLOOS, W. 2002 Large-scale finite-wavelength modulation within turbulent shear flows. *Phys. Rev. Lett.* **89** (1), 014501.
- SCHUMACHER, J. & ECKHARDT, B. 2001 Evolution of turbulent spots in a parallel shear flow. *Phys. Rev. E* **63** (4), 046307.
- SKUFCA, J. D., YORKE, J. A. & ECKHARDT, B. 2006 Edge of chaos in parallel shear flow. *Phys. Rev. Lett.* **96**, 174101.
- TILLMARK, N. & ALFREDSSON, P. H. 1992 Experiments on transition in plane Couette flow. *J. Fluid Mech.* **235**, 89–102.
- TSUKAHARA, T., SEKI, Y., KAWAMURA, H. & TOCHIO, D. 2005 DNS of turbulent channel flow at very low Reynolds numbers. In *Proceedings of the 4th International Symposium on Turbulence and Shear Flow Phenomena*, pp. 935–940. Begel House.
- VAN ATTA, C. 1966 Exploratory measurements in spiral turbulence. *J. Fluid Mech.* **25** (03), 495–512.